Journal of Energy Storage 56 (2022) 105889

Contents lists available at ScienceDirect

Journal of Energy Storage

journal homepage: www.elsevier.com/locate/est

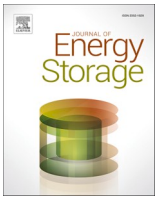

Research Papers

Transition to a low-carbon building stock. Techno-economic and spatial optimization of renewables-hydrogen strategies in Spain

V.M. Maestre, A. Ortiz, I. Ortiz *

Chemical and Biomolecular Engineering Department, ETSIIyT, Universidad de Cantabria, Av. los Castros s/n, 39005 Santander, Spain

ARTICLE INFO

Keywords:
Renewable hydrogen-based systems
Low-carbon electricity supply
Spanish building stock
Centralized vs distributed
Techno-economic optimization
Land eligibility

ABSTRACT

Europe has set ambitious targets to reduce the final energy consumption of buildings in concerning the degree of electrification, energy efficiency, and penetration of renewable energy sources (RES). So far, hydrogen is becoming an increasingly important energy vector, offering huge opportunities to promote the share of intermittent RES. Thus, this manuscript proposes an energy model for the complete decarbonization of the estimated electricity consumed by the Spanish building stock in 2030 and 2050 scenarios; the model is based on the combination of photovoltaic and wind primary sources and hydrogen technologies considering both distributed and centralized configurations, applying also geospatial criteria for their optimal allocation. Large-scale RES generation, centralized hydrogen production, and re-electrification, along with underground hydrogen storage, result in the lowest levelized cost of energy (LCOE), hydrogen production costs (HPC), and the highest overall efficiency (μ_{SYS}). Wind energy is mainly harvested in the north of Spain, while large PV farms are deployed in the mid-south. Furthermore, reinforcement of underground hydrogen storage enhances the overall system performance, reducing surplus energy and the required RES generation capacity. Finally, all the considered scenarios achieve LCOE below the Spanish utility grid benchmark, apart from accomplishing the decarbonization goals established for the year 2030.

1. Introduction

The unsustainable climate situation generated by fossil fuel-based energy production has increased the urgency to implement an energy model based on renewable energy sources (RES) [1]. However, their intermittent nature requires large and durable energy storage systems (ESS) [2]. In this regard, hydrogen has been appointed as a feasible and versatile energy carrier that can be produced during peak power generation periods [3], stored seasonally [4], and then employed to decarbonize different economic sectors [5] from recovered waste streams [6], replacing fossil fuels [7], used as feedstock [8] or purified from industrial activities [9], or for heat and power generation [10,11].

So far, different works have modeled theoretical scenarios where high penetration of RES-hydrogen infrastructures are evaluated to ensure a low-carbon energy supply in Europe. Caglayan et al. [12] analyzed the supply with 100 % RES and hydrogen infrastructure in Europe to design the required hydrogen pipelines and electricity transmission network through a multi-year analysis. Moreover, they studied the potential capacity of salt caverns in Europe to store the hydrogen required for the energy transition to a low-carbon supply system. Moser et al. [13] integrated a variety of ESS and their prospected evolution to optimize the system costs and distribution of the transmission network, performing a sensitivity analysis on the CAPEX of converter and storage. Pavičević et al. [14] studied the need for sector coupling to ensure the flexibility of the European energy system with high RES penetration. Child et al. [15] provided a detailed evaluation of two different scenarios of 100 % RES in Europe: considering each country independently or assuming transmission interconnections between regions. Löffler et al. [16] accounted for the possible risks of creating stranded assets during the energy transition in case of lack of planning. The model considered electricity, heating, and transportation sectors in different scenarios during the 2015–2050 period. Furthermore, different storage methods such as lithium-ion or redox-flow batteries, pumped hydro, compressed air, hydrogen, and methane are analyzed. Likewise, Zappa et al. [17] analyzed the feasibility of a 100 % RES European power system by 2050 with modeling and optimization of the size and geographical distribution of generation facilities, including the prospected electricity requirements to generate green hydrogen.

Likewise, several reported studies have evaluated the potential use of hydrogen as seasonal energy storage system in different countries of Europe, as well as global trading routes from countries with abundant

* Corresponding author.
E-mail addresses: maestrevm@unican.es (V.M. Maestre), ortizal@unican.es (A. Ortiz), ortizi@unican.es (I. Ortiz).

https://doi.org/10.1016/j.est.2022.105889
Received 22 August 2022; Received in revised form 13 October 2022; Accepted 15 October 2022
Available online 21 October 2022

Abbreviations

ANL	Argonne National Laboratory
BNEF	BloombergNEF
CAPEX	Capital Expenditures
CCSU	Carbon Capture, Storage and Utilization
CF	Capacity Factor
CHP FC	Combined Heat & Power Fuel Cell
CO_2	Carbon Dioxide
EL	Electrolyzer
EMEA	Europe, The Middle East and Africa region
ESS	Energy Storage System
FC	Fuel Cell
GLAES	Geospatial Land Availability for Energy Systems
H_2	Hydrogen
HDSAM	Hydrogen Delivery Scenario Analysis Model
HOMER Pro	Hybrid Optimization of Multiple Energy Resources Professional
HPC	Hydrogen Production Cost, US$/kg
IEA	International Energy Agency
LCOE	Levelized Cost of Energy, US$/kWh
MgH_2	Magnesium Hydride
MgO	Magnesium Oxide
NPC	Net Present Cost
NREL	National Renewable Energy Laboratory of the United States
OPEX	Operational Expenditures
PEMEC	Proton Exchange Membrane Electrolyzer
PEMFC	Proton Exchange Membrane Fuel Cell
PV	Photovoltaic
RES	Renewable Energy Sources
RHS	Renewable Hydrogen-based Systems
WT	Wind Turbine
μ_{SYS}	System efficiency, %

Case studies

CEN1	Centralized base scenario
CEN2-SV	Centralized with compressed H_2 stored in steel vessels
CEN3-SC	Centralized with compressed H_2 stored in salt caverns
CEN4-CP	Centralized with compressed H_2 stored in salt caverns and distribution in pipelines
DIS1-PVB	Distributed base scenario (with rooftop PV and batteries)
DIS2-PVBC	Distributed with compressed H_2 stored in steel vessels
DIS3-PVSC	Distributed with compressed H_2 stored in salt caverns
DIS4-FCB	Distributed with Combined Heat & Power Fuel Cell and H_2 distribution in pipelines
DIS5-SV	Distributed with Combined Heat & Power Fuel Cell, compressed H_2 stored in steel vessels and distribution in pipelines
DIS6-SC	Distributed with Combined Heat & Power Fuel Cell, compressed H_2 stored in salt caverns and distribution in pipelines

renewable resources to those with high energetic requirements. Welder et al. [18] carried out a spatio-temporal optimization of the energy system required to cover industrial and mobility demands in Germany using hydrogen and power-to-gas facilities for energy storage. Likewise, Grüger et al. and Reuß et al. [19,20] compared different hydrogen infrastructure technologies for transport applications. Guandalini et al. [21] established a similar case study for Italy aiming at decarbonizing the electricity generation sector. Subsequently, they compared the results with the ones obtained with different energy models in Germany. Samsatli et al. addressed the potential transition of transport [22] and heat sectors [23] in the UK by combining wind turbines and hydrogen storage. Furthermore, Tlili et al. [24] assessed the possibilities to increase RES penetration and reduce the prominent role of nuclear power in France by simulating and comparing both an isolated and interconnected French scenario to assess the potential hydrogen capacity that could be generated from electricity surpluses in 2035. Heras et al. [25] studied the substitution of current power facilities with renewable hydrogen-based systems (RHS) to cover the baseload production in Spain. This work employed magnesium for hydrogen storage in the form of solid magnesium hydride (MgH_2). Then hydrogen is released by reacting with water, generating pure hydrogen and magnesium oxide (MgO). The work additionally compares the energetic needs of the system with and without magnesium oxide (MgO) regeneration. Furthermore, Heuser et al. [26] performed a techno-economic analysis of the potential hydrogen trade between Japan and the region of Patagonia (Argentina and Chile). Additionally, the geographical distribution and location of hydrogen energy generation, production, and storage systems have been the subject of study in recent years. In particular, Ryberg et al. [27,28] have developed a model to determine the area available at a given region for the location of solar panels and wind turbines considering different exclusion criteria such as socio-political, physical, economic, and conservation of nature. For instance, this model has been employed for the assessment of onshore wind turbines deployment in Europe [29].

Most of the analyzed references so far, study the possibilities of decarbonizing hard-to-abate sectors such as industry or transportation, as well as evaluating the possible use of RHS in microgrids, addressing their control [30], design [31] and operation [32]. Other works are assessing the potential use of reversible fuel cells (specially solid oxide ones), that are being simulated for microgrid heat and power supply [33] and studied at prototype scale [34], with ultimate targets for 2050 of achieving roundtrip efficiencies over 70 % (including thermal energy), and competitive costs and lifetimes [35]. However, few of the reported articles focus on the residential and buildings sector, which is responsible for around 40 % of the final energy consumed in Europe [36,37]. Moreover, this assessment has not been carried out so far at country level in Spain, which is the fourth most populated country of the European Union with around 47 million inhabitants. Geographically, Spain is in the southwest of Europe and is characterized by a huge PV potential (particularly in the south of the country) combined with relevant wind possibilities in the north, in several mountain chains across the country, and the surroundings of the Strait of Gibraltar. Furthermore, the low density of population in some regions of Spain increases the land eligible for the deployment of large renewable generation hubs. Moreover, other technologies such as concentrated solar power or novel floating offshore wind turbines could play a relevant role in the upcoming years.

In this sense, this work addresses the decarbonization of the Spanish building stock as a case study, carrying out a geospatial assessment of the available territory to reduce the size of additional wind farms and solar parks to be installed. The main objective of this research is the accomplishment of the optimal renewables-hydrogen configurations in terms of levelized cost of energy (LCOE), hydrogen production costs (HPC) [38], and overall efficiency to decarbonize the Spanish building stock, together with the definition of the most suitable and profitable locations of RES generation hubs and hydrogen technologies throughout the country. For this purpose, several case studies are evaluated combining large-scale renewable energy production with hydrogen chain alternatives. Although liquid [39] and solid [40]hydrogen storage are being considered to improve the volumetric density of hydrogen, these configurations include different gaseous hydrogen storage methods such as steel tanks, underground storage in salt caverns [41],

hydrogen pipelines, and their combinations [42] apart from two alternatives of power retrieval in multi-MW PEM fuel cells [43] or small/medium-scale cogeneration fuel cell units deployed in buildings [44]. The analysis on a country basis will provide greater robustness and detail to the results obtained, apart from enabling their comparison with the objectives defined by the long-term decarbonization strategy of Spain [45]. Besides, the proposed methodology has the advantage that it can be extended to different regions or countries, by introducing the required electricity demand profile and climate conditions at a given location along with the eligibility of the region subject of study.

2. Methodology

This section briefly describes the techno-economic and spatial analysis carried out on a country basis within this research work, including the modeling software, the electricity demand of the Spanish building stock (excluding those in Balearic and Canary Islands), the cost and characteristics of the main technologies considered for the optimization, and the case studies analyzed. The problem addressed in this paper has the ultimate goal of achieving the lowest levelized cost of energy (LCOE) through a configuration that is based on wind and photovoltaic RES as the primary energy source, hydrogen production via water electrolysis, seasonal hydrogen storage, and power retrieval in fuel cells to cover the electricity needs of the Spanish building stock in 2030 and 2050 time spans. Besides, this study evaluates the geo-spatial distribution of RES generation hubs within the Spanish territory along with the allocation of hydrogen technologies. The methodology framework proposed and followed in this manuscript is depicted in Fig. 1.

This methodology is divided into three stages: 1) input data inventory, 2) definition of the objective function and computational tools employed, and 3) analysis and evaluation of the results. The first stage requires the estimation of the electrical load to be covered by RES and the hydrogen chain as well as the estimated compressor consumption. Thus, the consumption has been distributed proportionally by autonomous community and the load profile varies according to the climate zones defined by the Spanish Institute for Energy Diversification and Saving (IDAE) [46]. Then, the meteorological information of Spain is considered along with the land eligible to place the generation facilities, together with the equipment costs and characteristics. In this regard, restrictive criteria have been defined concerning wind speed and solar irradiation to obtain the optimal locations of renewable energy sources, being the climate conditions of the eligible areas the ones selected in each region for the simulations in HOMER Pro. Apart from minimizing LCOE, main objective in the present study, the selection of the most suitable locations to deploy renewables-hydrogen configurations has been investigated. Furthermore, the balance between the minimum hydrogen production costs (HPC) and the maximum system efficiency (μ_{SYS}) has been considered to obtain the most favorable implementation. HOMER Pro has been employed for the techno-economic optimization and GLAES based on Python programming to get land eligibility. In addition to these outcomes, the electricity mix composition has been obtained for every case study. The evaluated scenarios have been compared based on the above parameters. Moreover, different solutions have been proposed to enhance the system performance by harnessing energetic surpluses.

2.1. Computational tools

This section briefly describes the tools HOMER Pro and GLAES, that have been used to perform the techno-economic and spatial analysis.

2.1.1. HOMER Pro software

HOMER Pro software (acronym of Hybrid Optimization of Multiple Energy Resources) [47] was developed by the National Renewable Energy Laboratory (NREL) of the United States. This tool enables the user to calculate the optimal size of the target system with the objective function of minimizing the levelized cost of energy (LCOE) and the net present cost (NPC). It has been employed during the last decade to optimize the energy system for multiple stationary applications such as remote areas [48], microgrids [49], homes [50], commercial or research buildings [51,52], sports complexes [53], reverse osmosis desalination plants [54] or mines [55].

In this work, HOMER Pro has been employed to define the system required to decarbonize the electricity consumption of the Spanish building stock in 2030 and 2050. The average daily load, for both 2030 and 2050 time horizons, is entered and then distributed hourly, defining peak and off-peak periods. The compressor consumption is included in the average daily load. At the same time, the climate conditions (solar resources, average wind speed, and temperature) of Spain are downloaded from NASA databases. Subsequently, all the components are modeled by introducing their costs (CAPEX, OPEX, and replacement), and characteristics (lifetime, efficiency, temperature effects, and degradation). As a result, different possible configurations are simulated and optimized, being classified, and ranked according to the lowest LCOE and NPC. The main results of the simulations consist of the capacities of the components, LCOE, NPC, and the electricity mix

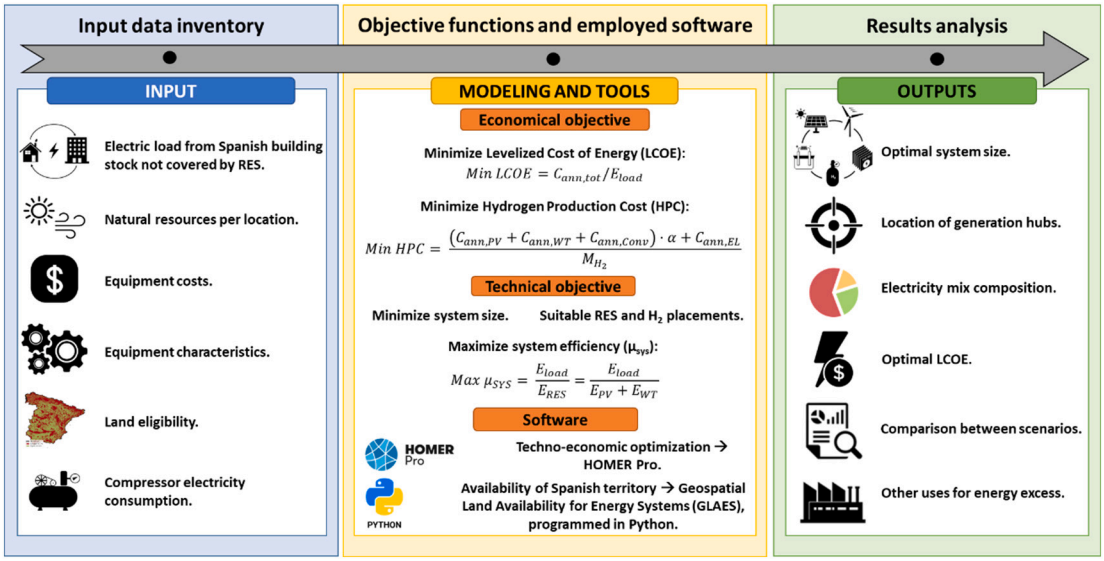

Fig. 1. Methodology framework for the proposed model.

composition. Moreover, this tool provides a detailed report of every component included in the system, evaluating several additional parameters such as hours of operation, maximum, minimum and average power delivered or consumed, hydrogen production and consumption, or hourly distribution of the generation among others.

2.1.2. Land eligibility

Land availability plays a crucial role in the deployment of energy systems. Thus, their implementation is not only subjected to their techno-economic competitiveness, but to several constraints and criteria for an effective evaluation of whether the technology in question is allowed to be placed at a given location. In this regard, the land eligibility of the energy systems obtained in HOMER Pro and discussed herein is based on a program developed in the Python programming language named Geospatial Land Availability for Energy Systems (GLAES). This program developed by Forschungszentrum Jülich GmbH can be found on GitHub as open source [56]. It covers four generalized criteria to assess the availability of a defined spatial region: physical, sociopolitical, conservation, and economic criteria [57,58]. Depending on how restrictive one wishes to be concerning the main criteria defined above, low, typical, or high exclusion values are set. These criteria determine the surface of Spain that is excluded in relation to the proximity of the generation hub to infrastructure such as roadways or power lines; protected areas, like wildernesses, or biospheres; and geological formations (rivers, lakes, coasts, woods, etc.). Likewise, regions that do not achieve a minimum value of average wind speed or direct normal irradiance are dismissed [27]. In this work, low exclusion criteria have been set as it has been assumed a political, social, and economic framework that favors the achievement of the decarbonization objectives in the 2030 and 2050 time horizons. These criteria are collected in the *Supplementary Information sheet, section S2.1*.

2.2. Definition of the energy demand

The buildings sector in Spain (accounting for residential, commercial, public administration, and buildings for different services) is responsible for around two-thirds of the total electricity consumption in the country, while the other third is mainly related to industrial activities [59]. Due to the climatic characteristics of Spain, the contribution of electricity to the total energy consumption in buildings is higher than that of heating compared with other countries in Europe, representing a more favorable scenario for the use of hydrogen as energy carrier for RES surplus seasonal storage [46]. Hence, the total electricity consumption in Spain in 2019 was around 234.5 TWh of which 147.6 TWh corresponded to the building stock [59]. Regarding electricity generation, 37.2 % of the total production (275.8 TWh) came from renewables [60]. Considering the same percentage between generation and final electricity consumption in all the sectors, despite differences due to transmission losses, exported and imported energy or mismatches between generation and demand, it turns out that about 55 TWh of electricity consumed by buildings comes from renewable sources.

Regarding future consumption forecasts for the years 2030 and 2050, different scenarios depending on the degree of compliance with the Paris agreement and the required energy transition may be considered. Within the most ambitious decarbonization scenario whereby global warming is limited to 1.5 °C above pre-industrial levels, electrification rates of 68 % and 51 % are set for residential and service buildings respectively in 2030, while 74 % and 100 % are required in 2050 [61]. In this scenario, the total electricity demand of the Spanish building stock would be 162 TWh in 2030 and 240 TWh in 2050. However, there are already 55 TWh of electricity that are covered with RES, so the newly designed energy systems based on RES, hydrogen generation, storage, and power retrieval in fuel cells are sized to cover 107 TWh and 185 TWh in 2030 and 2050, respectively. More details of the demand modeling are given in the *Supplementary Information sheet, section S1.8*.

2.3. Description of the system components

The size, distribution, and layout of the components within the Spanish territory are highly impacted by the characteristics of the technologies and their planned evolution in the 2030 and 2050 time horizons. Therefore, Table 1 gathers the forecasted range of capital expenditures (CAPEX), operational expenditures (OPEX), and replacement costs of the equipment along with the main characteristics considered in the simulation of the energy system. The lower limit of CAPEX ranges has been selected for the simulations under the hypothesis of a favorable policy framework for the development of the different technologies.

The energy systems are designed to cover the previously depicted load demands by employing new additions of photovoltaic (PV) panels and wind turbines (WT) as primary RES. Whenever renewable surpluses from PV panels and WT are available, they are converted into hydrogen in proton exchange membrane electrolyzers (PEMEC) and stored at different pressure and through different methods. Moreover, batteries could also be used as an alternative or a complementary solution for short-term energy storage. Finally, if renewable energy is not sufficient to fulfill the energy requirements, proton exchange membrane fuel cells (PEMFC) are employed for power retrieval. To guarantee the appropriate flow of electricity throughout the electricity network and its signal quality (in terms of voltage and frequency) it is necessary to deploy different electrical sub-stations and power electronics. Thus, electricity is properly transmitted from large RES generation hubs to the load and is also adapted to the voltage, current, and frequency required by electrolyzer stacks for hydrogen generation. All these components are modeled in HOMER Pro software and the detailed models are provided in the *Supplementary Information sheet, section S1*.

Hydrogen compressors are employed to reduce the storage volume of the hydrogen produced in PEMEC. Thus, technological differences associated to the number of stages required and hydrogen pressure leaving the electrolyzer are considered. Moreover, the storage method (steel vessel, salt cavern, or pipeline) determines the target outlet pressure. The energy consumption of the compressor has been estimated through the Hydrogen Delivery Scenario Analysis Model (HDSAM) developed by the Argonne National Laboratory (ANL) of the US National Renewable Energy Laboratory (NREL) [74,75], according to Eqs. (1) and (2):

$$Power, kW = (Z)(\dot{m})(R)(T)(n)\left(\frac{1}{\eta}\right)\left(\frac{k}{k-1}\right)\left[\left(\frac{P_{outlet}}{P_{inlet}}\right)^{\left(\frac{k-1}{n\cdot k}\right)} - 1\right] \quad (1)$$

$$z = \frac{z_2}{z_1} ln\left(\frac{z_2}{z_1}\right) \quad (2)$$

where z is the mean compressibility factor of hydrogen; z_1 and z_2 are the compressibility factors of hydrogen at the compressor inlet and outlet, respectively [76]; $\dot{m}$ is the mass flow rate of hydrogen (kg/s); R is the universal constant, 8.3144 kJ/kg-mole-K; T is the inlet hydrogen temperature (K); n is the number of stages; η is the isentropic efficiency, 88 %; k is the isentropic exponent of hydrogen ($k = 1.4$); P_{outlet} and P_{intlet} are the outlet and inlet pressures of the compressor respectively.

As HOMER Pro software does not include hydrogen compressor in its components library, it has been calculated by introducing the electrolyzer generation profile in Eq. 1. Hence, it results in the compressor consumption that is simulated along with the building stock demand.

2.4. Case studies

The future decarbonization of the buildings sector in Spain can be adapted to different configurations. In this regard, a variety of possible future alternatives is presented in Fig. 2 to assess the cost-effectiveness and dimensions of the case studies. Every scenario considers large-scale RES generation through the combination of PV panels and WT.

Table 1
Equipment costs and main characteristics.

Year	Component	Technology	Costs			Equipment characteristics	Ref.
			CAPEX (US $/kW)	Replacement (US $/kW)	OPEX (US $/kW)	Description	
2030	PV	Large scale	550–800	50 % CAPEX	5 % CAPEX	Lifetime: 25 years. Derating factor: 85 %	[62–65]
		Rooftop	1100–1300	50 % CAPEX	5 % CAPEX		
	Wind turbine	On-shore	1100–1300	75 % CAPEX	2 % CAPEX	Lifetime: 22 years. Rated capacity: 7.58 MW (Enercon E-126). Hub height: 135 m. Rotor diameter: 127 m.	[62,66]
	Fuel Cell	PEMFC	800–1100	40 % CAPEX	5 % CAPEX	Lifetime: 80,000 h. Efficiency: 54 %.	[4,8,67,68]
		CHP FC	2000–2500	25 % CAPEX	4 % CAPEX	Fuel consumption: 0.055 kg/kWh	
	Electrolyzer	PEMEC	800–1100	30 % CAPEX	2 % CAPEX	Lifetime: 20 years. Efficiency: 48 kWh/kg. Outlet pressure: 60 bar.	[8,11,67,69]
	Hydrogen storage (US$/kg)	Steel vessel	500–650 (100–130)[a]	85 % CAPEX	1 % CAPEX	Lifetime: 25 years. Storage pressure: 60 bar (300 bar when compressed)	[67,70]
		Salt cavern	30–60	50 % CAPEX	10 % CAPEX	Lifetime: 50 years. Storage pressure: 120 bar with compression.	
		Salt cavern + pipeline	550–650	50 % CAPEX	10 % CAPEX	Lifetime: 50 years (pipelines, 25 years). Storage pressure: 120 bar with compression.	
	Battery (US$/kWh)	Li-Ion	400–600	100 % CAPEX	1 % CAPEX	Lifetime: 15 years. Roundtrip efficiency: 90 %	[71]
	Compressor	Mechanical	700–900	85 % CAPEX	5 % CAPEX	Lifetime: 20 years. Isentropic efficiency: 88 %.	[67,72]
	Power conversion		500–700	85 % CAPEX	5 % CAPEX	Lifetime: 25 years. Efficiency: 95 %	[73]
2050	PV	Large scale	400–600	50 % CAPEX	4 % CAPEX	Lifetime: 25 years. Derating factor: 90 %	[62–65]
		Rooftop	800–1000	50 % CAPEX	4 % CAPEX		
	Wind turbine	On-shore	900–1100	75 % CAPEX	2 % CAPEX	Lifetime: 25 years. Rated capacity: 7.58 MW (Enercon E-126). Hub height: 135 m. Rotor diameter: 127 m.	[62,66]
	Fuel cell	PEMFC	600–800	40 % CAPEX	5 % CAPEX	Lifetime: 100,000 h. Efficiency: 60 %. Fuel consumption: 0.045 kg/kWh	[4,8,67,68]
		CHP FC	1000–1400	25 % CAPEX	4 % CAPEX		
	Electrolyzer	PEMEC	200–600	30 % CAPEX	2 % CAPEX	Lifetime: 25 years. Efficiency: 43.8 kWh/kg. Outlet pressure: 70 bar	[8,11,67,69]
	Hydrogen storage (US$/kg)	Steel vessel	425–550 (100–130)[a]	85 % CAPEX	1 % CAPEX	Lifetime: 25 years. Storage pressure: 70 bar (300 bar when compressed)	[67,70]
		Salt cavern	30–60	50 % CAPEX	10 % CAPEX	Lifetime: 50 years. Storage pressure: 120 bar with compression.	
		Salt cavern + pipeline	550–650	50 % CAPEX	10 % CAPEX	Lifetime: 50 years (pipelines, 25 years). Storage pressure: 120 bar with compression.	
	Battery (US$/kWh)	Li-Ion	300–500	100 % CAPEX	1 % CAPEX	Lifetime: 17 years. Roundtrip efficiency: 90 %	[71]
	Compressor	Mechanical	600–800	85 % CAPEX	5 % CAPEX	Lifetime: 22 years. Isentropic efficiency: 88 %.	[67,72]
	Power conversion		400–600	85 % CAPEX	5 % CAPEX	Lifetime: 25 years. Efficiency: 95 %	[73]

Abbreviations: CAPEX (Capital Expenditures), OPEX (Operational Expenditures), PV (Photovoltaic), PEMFC (Proton Exchange Membrane Fuel Cell), CHP (Combined Heat and Power Fuel Cell), PEMEC (Proton Exchange Membrane Electrolyzer Cell).
[a] CAPEX costs for hydrogen storage in steel vessels when compressed to 300 bar.

However, the hydrogen supply chain varies from centralized to distributed scenarios to evaluate whether the best alternative is to produce, store and consume hydrogen in large-scale facilities or distribute hydrogen through dedicated and/or repurposed pipelines to end users for in situ power retrieval in domestic fuel cells. Thus, the case studies have been organized and named as follows:

a) Centralized scenarios: include large-scale RES generation, large-scale hydrogen production, compression, and storage in different methods along with hydrogen re-electrification in large fuel cells. Only electricity is transmitted to buildings. The baseline scenario (CEN1) considers storage in steel vessels without compression, while CEN2-SV considers compression to reduce the volume and number of steel tanks. Additionally, two scenarios considering hydrogen compression and storage in salt caverns are analyzed, but they differ in whether the hydrogen is consumed in fuel cells next to the salt caverns (CEN3-SC) or the fuel cells are separated from the storage, requiring hydrogen distribution (CEN4-CP).
b) Distributed scenarios: as for centralized ones, these include large-scale RES generation, but PV panels on the rooftop of buildings are considered to reduce the land footprint of large PV parks. Furthermore, batteries are also evaluated as a complementary solution for short-term energy storage. The use of batteries as energy storage system has been limited to distributed scenarios for different reasons: loss of energy storage capacity over time due to degradation of large Li-ion batteries, lithium high growth forecast in future demand (more than 40 times by 2040 compared to 2020), and high geographical concentration of this mineral from both a production and processing perspective [77]. Among distributed scenarios, their main differences come from the hydrogen value chain. In three cases hydrogen is produced, stored, and used for re-electrification in large facilities. Hydrogen is stored directly from the outlet of PEMEC and stored in steel vessels (DIS1-PVB), being previously compressed and stored in steel tanks (DIS2-PVBC) or salt deposits (DIS3-PVSC). For the remaining scenarios, hydrogen is generated in multi-MW electrolyzers and it can either be stored in steel vessels without (DIS4-FCB) and with compression (DIS5-SV) or compressed in salt caverns (DIS6-SC). In these last scenarios, hydrogen is distributed and transmitted for its consumption in combined heat and power fuel cells that are installed in every building.

3. Results and discussion

The results obtained in this study using the aforementioned methodology are described and discussed in this section to analyze the techno-economic capabilities of renewable energies and hydrogen-

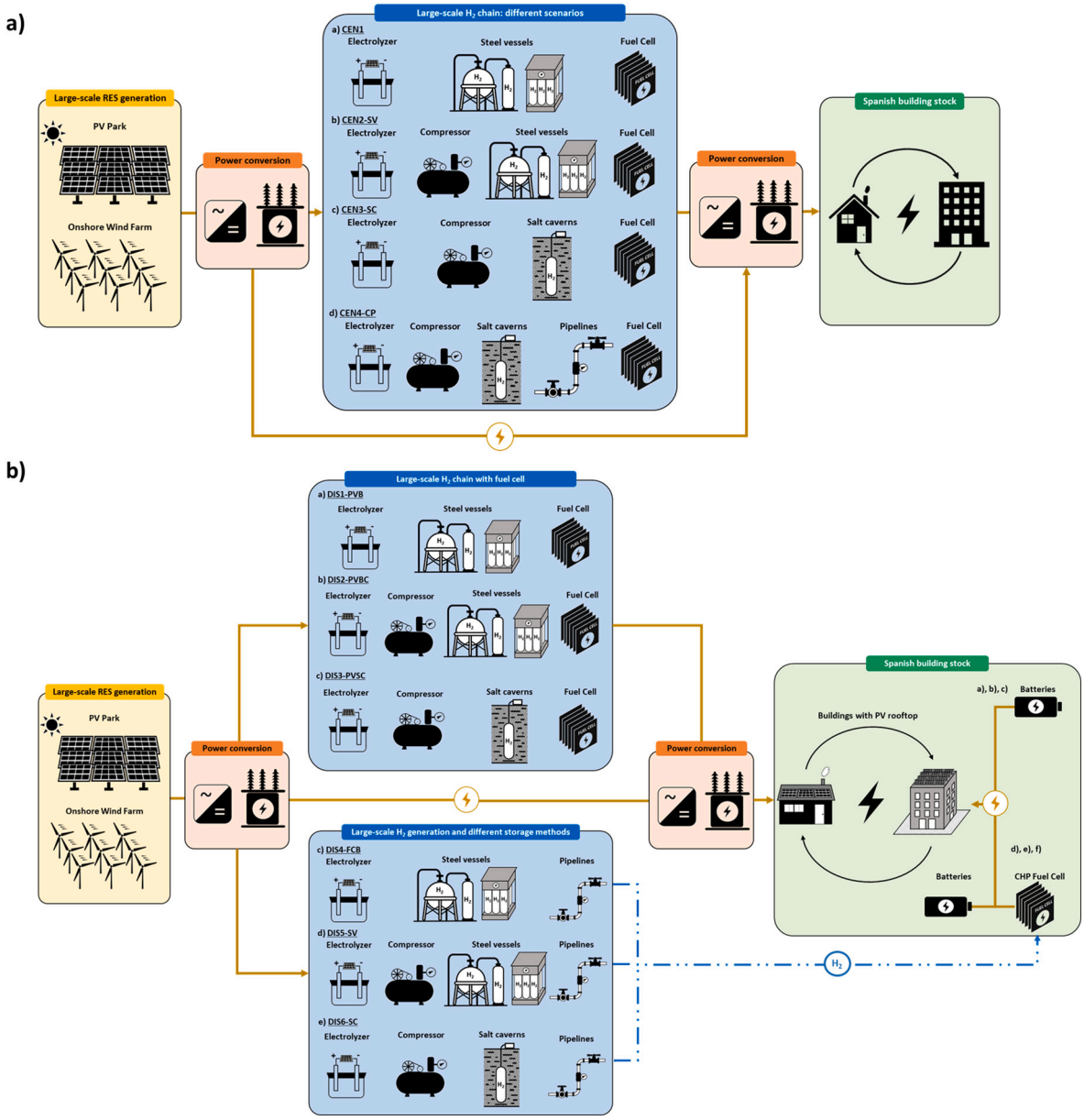

Fig. 2. Case studies simulated to achieve the Spanish building stock decarbonization: a) Centralized vs b) distributed scenarios.

based technologies to cover the electricity demand of the Spanish building stock. Moreover, the geospatial distribution of energy generation hubs within the Spanish territory is displayed. Finally, possible uses of energy excess and alternatives to enhance the energy performance of the systems are evaluated.

3.1. Centralized scenarios (2030 & 2050)

Fig. 3a depicts the generation, conversion, and required storage capacities per centralized scenario to cover the Spanish building stock demand in both 2030 and 2050 horizons. By the end of 2020s decade, the predominant RES will be wind energy, growing up to 47.4 or 53.7 GW depending on the scenario. The characteristics of the energy demand in buildings (higher consumption during evening/night) makes wind energy profile more suitable, as the capacity factor and the hours of operation are higher than those for PV panels. This results in a lower LCOE for wind energy than for PV energy. The predominance of wind energy as main renewable source in Spain has been already forecasted by the Spanish Government in the Integrated Energy and Climate Strategy [78].

However, in 2050, photovoltaic energy will experience the greatest increase (between 75 % and 90 % of installed capacity in 2030 except for the CEN3-SC scenario), even surpassing the power of wind generators in the CEN2-SV scenario (68.8 and 62.9GW respectively). The development of PV panels, along with the great solar potential of Spain, will contribute to the rapid growth in the deployment of photovoltaic energy in 2050. In addition, considering that the PV generation profile could better cover the demands of other sectors such as industry and transportation will promote the deployment of this technology across the country.

Regarding the electrolyzer, the fuel cell, and the required hydrogen storage capacities, all of them reflect the same values for every scenario since the demand to be covered is constant. The required installed PEMEC capacity in 2030 is 33 GW, 26 GW of PEMFC, and 63,000 t of hydrogen storage capacity (equivalent to 2100 GWh); while in 2050, these dimensions rise to 65 GW, 45 GW, and 87,000 t (equivalent to 2900 GWh).

It can be noted that the installed capacity of compressors is below

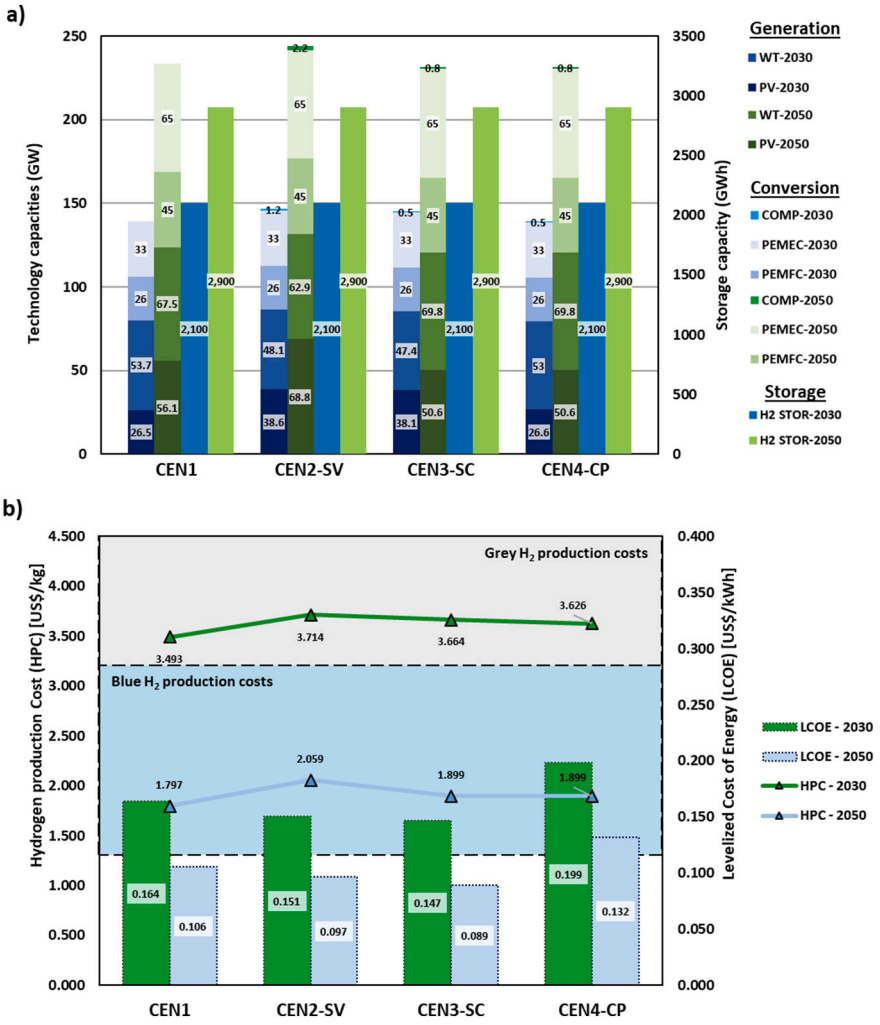

Fig. 3. a) Variation of generation, conversion (GW), and storage capacities (GWh) for centralized scenarios in 2030 and 2050; b) Hydrogen production costs (HPC) in US$/kg and levelized cost of energy (LCOE) in US$/kWh for centralized scenarios in 2030 and 2050. Blue and grey hydrogen production costs are based on [79]. (For interpretation of the references to colour in this figure legend, the reader is referred to the web version of this article.)

1.5 % of RES capacity in every scenario and time horizon, with energy consumptions always below 3 % of that required for the Spanish building stock. The comparison between base scenario CEN1 and CEN2-SV (same case study including hydrogen compression to 300 bar) reflects the growth of renewable energy required capacity from 80.2 GW to 86.7 GW in 2030 (8 % increase) and from 123.6 GW to 131.7 GW in 2050 (6.5 % increase). Additionally, hydrogen storage in salt deposits without and with pipeline distribution (scenarios CEN3-SC and CEN4-CP) results in more efficient configurations regarding compression and RES requirements than CEN2-SV as lower pressure is needed (300 bar for steel vessels vs 120 bar salt deposits with and without distribution [70]). Besides, there are slight differences in the amount of hydrogen generated along one year even having the same hydrogen storage capacities (all the details of the simulations are provided in the *Supplementary data Excel sheet*). Therefore, it can be concluded that hydrogen compression has not had a major impact on configurations size as their electricity consumption is not very significant compared with the estimated buildings demand, and the extra renewable capacity is below 8 % in every case. Moreover, compressors contribute to reducing drastically the volume required for hydrogen storage. For instance, 4.9 kg/m^3 of hydrogen can be stored at 60 bar, while 24.6 kg/m^3 can be stored if hydrogen is compressed up to 300 bar.

Regarding economic competitiveness, Fig. 3b represents the levelized cost of energy (LCOE) and hydrogen production costs (HPC) per scenario in 2030 and 2050. Furthermore, ranges for prospected blue and grey hydrogen production costs are defined as the benchmark for the results obtained in this work. The ranges for both grey and blue hydrogen (from natural gas and coal) have been obtained from the "Global Hydrogen Review 2021" elaborated by the International Energy Agency (IEA) [79]. Grey hydrogen costs are forecasted between 1.3 and 6.5 US$/kg, while blue hydrogen is predicted from 1.2 to 3.2 US$/kg, depending on the region and the availability of fossil fuels. According to this report, current prices of grey hydrogen are about 0.50 US$/kg cheaper than those reflected for blue hydrogen with carbon capture, storage and utilization (CCSU). However, the pricing and penalties for CO_2 emissions from 100 to 200 US$/t in the mid and long term, make blue hydrogen more cost-effective. Furthermore, the price of natural gas has suffered an exponential growth due to inflation and Ukraine war, making green hydrogen already cheaper than grey one in Europe, the Middle East and Africa (EMEA) region, and China according to BNEF [80].

The most competitive scenario concerning LCOE is CEN3-SC where hydrogen is compressed and stored in salt caverns for both periods 2030 and 2050. This price is highly influenced by the low cost per kilogram of underground storage. Nonetheless, every scenario results in lower LCOEs than the current electricity price in Spain (0.326 US$/kWh as of December 2021) which is continuously increasing [81]. Concerning HPC, the most competitive scenario is the baseline as there is no

compression considered with the associated decrease in RES and power conversion needs. Despite these configurations are not intended for hydrogen generation, but for seasonal energy storage with demand-driven hydrogen re-electrification, in 2030 every scenario achieves HPCs in the range of grey hydrogen and comparable values to blue hydrogen in 2050.

Furthermore, Table 2 reflects the system efficiencies of the centralized scenarios for 2030 and 2050. In general, the development of renewables and hydrogen technologies will lead to an improvement on the overall performance from 2030 to 2050. In this regard, the systems storing hydrogen in salt deposits are the most efficient ones in both the 2030 and 2050 time horizons. Therefore, considering the obtained LCOE, HPC and efficiency, the most interesting configuration turns out from combining large-scale RES generation, hydrogen production, compression and storage in salt deposits, and power retrieval in large FCs (scenario CEN3-SC).

Fig. 4 represents the land eligibility of CEN3-SC case study for PV farms (Fig. 4a) and wind turbines (Fig. 4b), the RES capacity that has to be installed per province in 2030 (Fig. 4c) and 2050 (Fig. 4d) with the total capacity required by Autonomous Community represented in growing circles and the sharing between PV and WT, the required hydrogen storage capacity per province in 2030 (Fig. 4e) and 2050 (Fig. 4f) with the total capacity of PEMEC and PEMFC required by Autonomous Community represented with growing icons respectively.

The land eligibility shows a great availability for both PV panels and wind turbines deployment (exclusion criteria are summarized in the *Supplementary Information sheet, section S2.2*). The final distribution has been carried out to harness the eligible regions with greater direct normal irradiance and higher average wind speeds. Thus, the northern half of Spain holds mostly wind farms (except for Salamanca with great solar potential), while the southern half contains large PV farms (apart from Cadiz and Malaga provinces, with high average wind speeds). As the eligible zones for RES deployment widely surpass the building stock requirements, the distribution remains constant for 2050, but with the corresponding repower of RES capacities per region. Finally, regarding the hydrogen value chain, the provinces with wider underground storage potential reflected by HyUnder European project [82] are selected, with hydrogen generation and re-electrification hubs next to the storage facilities. These regions correspond to mountain ranges like Cantabrian, Iberian, Betic, or Sierra Morena. The Ebro Valley is another region with potential.

In total, Spain accounts for a huge capacity of up to 1260 TWh of hydrogen that can be stored in underground in salt caverns according to Caglayan et al. [83], making CEN3-SC a very attractive solution not only for buildings decarbonization but for other economic sectors like industry or transportation. However, although this great potential, it is still a technology under development that needs further testing and demonstration. Other formations like depleted oil and gas fields or aquifers are being studied as well [79,84].

3.2. Distributed scenarios (2030 & 2050)

Like in centralized scenarios, Fig. 5a shows the production, conversion, and required storage capacities per distributed case study to cover the Spanish building stock demand in both 2030 and 2050 time horizons. These scenarios reflect the same trend and predominance of wind energy, with a newly installed capacity between 47.8 and 51.1 GW for 2030, and growth between 64.9 and 70.5 GW for 2050 depending on the scenario. The main variations correspond to the addition of rooftop PV panels. According to the Spanish roadmap for PV self-consumption [85], the estimated capacity installable on the roofs of the Spanish building stock (considering those roofs that reflect techno-economic competitiveness) is 9 GW for 2030 and 15 GW for 2050. However, these data may change if the development of roof-mounted PV panels leads to greater economic savings than expected, in addition to the creation of measures and subsidies that favor both their installation and acceptance by end users. The large-scale adoption of PV self-consumption implies a minimization of the land footprint of renewables, harnessing the existing infrastructure to generate renewable energy. In this case, both rooftop and grounded PV panels double their capacity from 2030 to 2050, and in the DIS5-SV case study almost results in the same capacity as wind energy: 65.9 GW for WT and 64.8 for PV. Furthermore, the addition of batteries, sufficient in all the cases to cover the peak demand of buildings for one hour (29 GW peak load and 29 GWh battery capacity in 2030, 50 GW peak load and 50 GWh battery capacity in 2050), minimizes the hydrogen storage needs compared to centralized scenarios, especially for those including cogeneration fuel cells that can additionally harness the heat generated during operation to reduce heating energy consumption in buildings. For instance, a decrease from 63,000 t of H_2 for centralized scenarios to 50,000 t of H_2 for distributed scenarios with CHP FC in 2030 is appreciated.

Finally, the utilization of small and medium-sized CHP fuel cells along with the presence of pipelines for the transmission of hydrogen in the case of DIS4-FCB, DIS5-SV, and DIS6-SC affects the system configuration. In 2030, these scenarios reflect higher penetration of grounded PV panels and higher utilization of batteries due to the higher cost per kW of CHP fuel cells, which implies lower needs in terms of hydrogen production and storage. However, as wind energy has a slightly lower contribution to the energy mix, it is necessary to install higher capacity of cogeneration fuel cells to cover peak demands. In this case, the capacity factor of the fuel cell (calculated as the ratio between its average power delivered and installed capacity) is lower for DIS4-FCB, DIS5-SV, and DIS6-SC scenarios. Likewise, in 2050 the hydrogen storage requirements decrease, and the FC capacity increase due to the above reasons: higher contribution of PV panels and batteries, lower generation of wind turbines, and higher prices of hydrogen storage systems. Nevertheless, in this period, the electrolyzer capacity increases from 60 GW in DIS1-PVB, DIS2-PVBC, and DIS3-PVSC scenarios to 64 GW in the remaining case studies. The low prices of electrolyzers are reflected in the optimization, as in terms of costs it is more advantageous having a greater capacity of hydrogen production and less storage than vice versa.

From an economic point of view, the most competitive case study in terms of LCOE is the DIS3-PVSC. As for centralized scenarios, the low cost per kg of hydrogen stored in salt caverns results in the lowest LCOE, even lower than the CEN3-SC scenario in 2030 (0.142 vs 0.147 US $/kWh). In 2050 the centralized scenario results in a lower LCOE (0.093 vs 0.089 US$/kWh). All the distributed case studies outperform the Spanish utility grid LCOE, being below the 0.326 US$/kWh reflected in December 2021 [81]. However, the scenarios including pipelines to distribute the hydrogen to the different buildings (DIS4-FCB, DIS5-SV, and DIS6-SC) report an increase between 37 % and 45 % compared to the other configurations. Regarding the hydrogen production cost (HPC), the most competitive scenario is DIS1-PVB followed by DIS3-PVSC. As for centralized scenarios, in 2030 every scenario achieves HPCs comparable to grey hydrogen and in 2050 they will be competitive

Table 2
System efficiencies of centralized case studies.

Case study	CEN1		CEN2-SV		CEN3-SC		CEN4-CP	
Year	2030	2050	2030	2050	2030	2050	2030	2050
System efficiency (μ_{SYS})	45.2 %	53.9 %	45.0 %	52.3 %	45.6 %	54.4 %	46.2 %	54.4 %

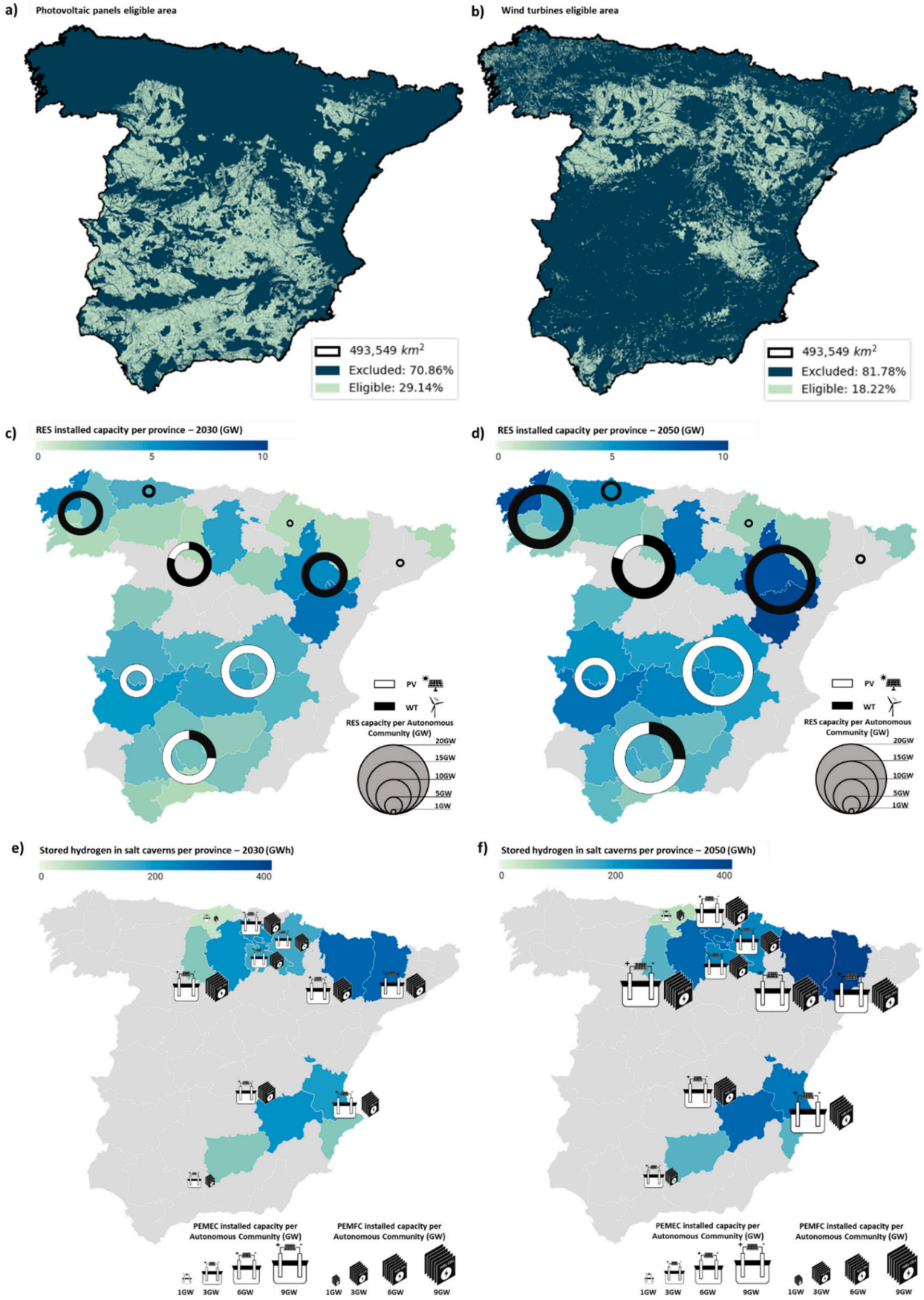

Fig. 4. Land eligibility for PV farms (a) and wind turbines (b), RES deployment (c and d), required hydrogen storage capacity in salt caverns, electrolyzers, and fuel cells layout (e and f) in 2030 and 2050 in Spain for scenario CEN3-SC.

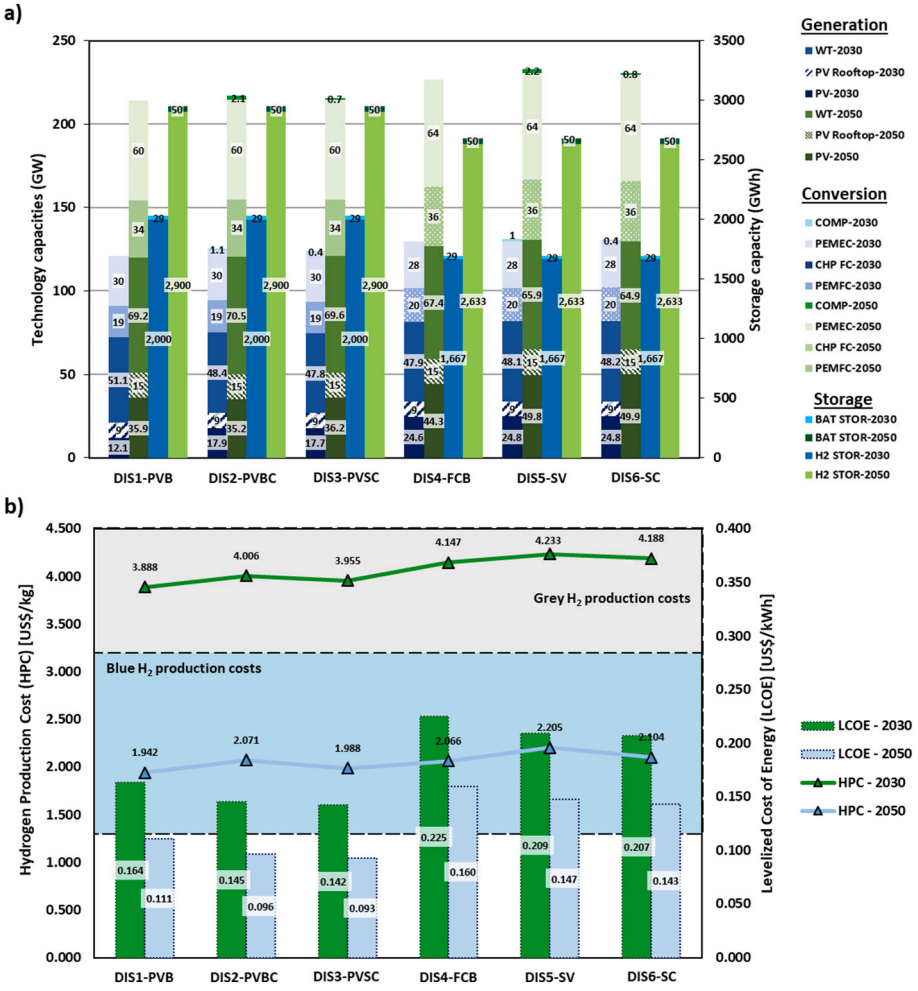

Fig. 5. a) Variation of generation, conversion (GW), and storage capacities (GWh) for distributed scenarios in 2030 and 2050; b) Hydrogen production costs (HPC) in US$/kg and levelized cost of energy (LCOE) in US$/kWh for centralized scenarios in 2030 and 2050. Blue and grey hydrogen production costs are based on [79]. (For interpretation of the references to colour in this figure legend, the reader is referred to the web version of this article.)

with blue hydrogen. In general, centralized scenarios show a better performance in HPC related to the presence of rooftop PV panels, whose cost per kW is higher than grounded PV panels.

Regarding the efficiency, as reported in Table 3, the DIS3-PVSC scenario is also the most competitive one for 2030 and 2050, achieving greater efficiencies than any other centralized or distributed scenario. Thus, this scenario is the most advantageous of the distributed configurations.

Fig. 6 depicts the land eligibility, RES distribution, and hydrogen chain layout throughout the Spanish territory for DIS3-PVSC. As for centralized configurations, wind turbines are located in the northern half, while large PV farms are installed in the mid-south. However, the addition of both roof-mounted PV panels and batteries reduces the total RES capacity that must be installed for centralized cases. Moreover, it enhances a more distributed energy generation mix. Accounting for both the climate conditions and the number of buildings per Autonomous Community, those regions with more buildings such as the Community of Madrid, Andalusia, Catalunya, and the Community of Valencia show high penetration of self-consumption facilities (rooftop PV and batteries). Likewise, the layout of the hydrogen chain is analog to CEN3-SC, where hydrogen generation and re-electrification facilities are located close to salt caverns. The main difference is the reduction in hydrogen storage requirements due to the deployment of batteries. From the end users perspective, this solution also provides the possibility of applying for subsidies because of a legislative framework that favors energy efficiency measures and solar self-consumption in buildings, apart from benefiting from injecting back to the utility grid the excess that cannot be directly used or stored. Although the price of this user-generated energy is lower (due to the fact that it does not include taxes for network maintenance, electricity meter rental and the contracted power is still charged), consumers can see a significant reduction in their bills.

3.3. Possible uses of excess energy (2030 & 2050)

To ensure a 100 % decarbonized electricity supply to the building sector in Spain through combined RES and hydrogen systems, it is

Table 3
System efficiencies of distributed case studies.

Case study	DIS1-PVB		DIS2-PVBC		DIS3-PVSC		DIS4-FCB		DIS5-SV		DISC6-SC	
Year	2030	2050	2030	2050	2030	2050	2030	2050	2030	2050	2030	2050
System efficiency (μ_{SYS})	49.9 %	54.6 %	49.5 %	54.1 %	50.0 %	54.6 %	47.1 %	52.9 %	46.8 %	52.0 %	46.8 %	52.5 %

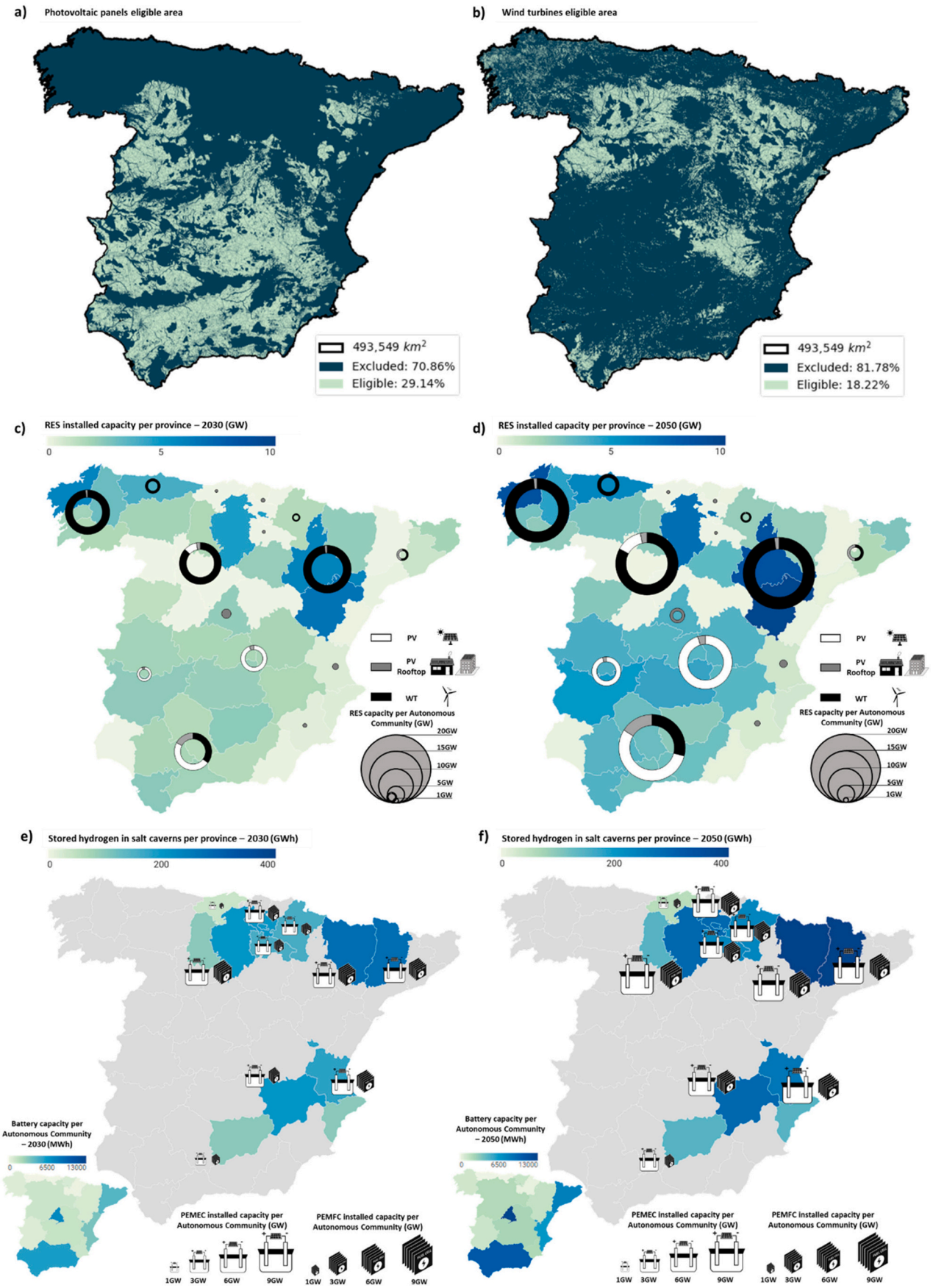

Fig. 6. Land eligibility for PV farms (a) and wind turbines (b), RES deployment (c and d), required hydrogen storage capacity in salt caverns, electrolyzers and fuel cells layout (e and f) in 2030 and 2050 in Spain for scenario DIS3-PVSC.

necessary to produce a large amount of energy that cannot or does not need to be fully stored. In this sense, the distributed case study DIS3-PVSC will be analyzed as it presents the best trade-off (slightly better than the resulting CEN3-SC configuration) in terms of energy costs and hydrogen production, as well as efficiency and profitability for end users. This configuration presents an energy excess of 64 TWh/year in 2030, which represents almost 60 % of the electricity demand of the building stock. Likewise, in 2050 this excess grows up to 95.1 TWh/year (51 % of the demand). Thus, this energy excess could be used to cover the electricity needs of other sectors such as industry, to generate more hydrogen, store more energy, or be exported to other countries.

3.3.1. Excess energy for industry (2030 & 2050)

As previously mentioned, the industrial sector is the other major electricity consumer, being responsible for almost the other third of the electricity demand in Spain. Thus, it is estimated that in 2030, the industry will require 105.6 TWh/year of electricity; while 139.5 TWh/year will be consumed in 2050 [61]. Assuming the 37.2 % of RES generation in Spain during 2019, the remaining electricity to be decarbonized is 65.9 TWh/year and 87.6 TWh/year in 2030 and 2050 respectively. Thus, the DIS3-PVSC configuration turns out in a slightly lower electricity excess than the total amount required to decarbonize the industrial demands in 2030 (64 vs 65.9 TWh/year), while in 2050, the surplus energy generated is higher than the remaining industrial demand (95.1 vs 87.6 TWh/year). However, these excesses do not correspond exactly to the industrial needs. To calculate how much electricity could be leveraged from the total surplus generated in each time span, both excess energy and industrial demand profiles are compared considering their corresponding hourly distribution. Thus, not all the excesses would be repurposed as they does not exactly match the industrial demand profile.

In 2030, only 20.6 TWh/year out of 64 TWh/year (32.2 %) can be used to partially cover the industrial needs, which represents around one third of the total demand. This improves the LCOE from 0.142 US$/kWh to 0.123 US$/kWh. Similarly, the excess electricity recovered in 2050 is 24.7 TWh/year, accounting for 25.9 % of the industrial electricity consumption. In this scenario, the LCOE slightly improves from 0.0927 US$/kWh to 0.0784 US$/kWh. The recovery values of electricity excess are so low because of the different characteristics of industrial and excess profiles. While industrial demand is almost constant throughout the day, the excess presents sharp peaks of production that quickly decrease to zero, as these correspond to residual energy from renewable sources. Therefore, it is very difficult to harness all the surpluses to cover just one sector given the differences between both profiles.

3.3.2. Excess energy for extra hydrogen production (2030 & 2050)

Another option to convert the great excess of energy produced into useful energy is the production of low-cost extra hydrogen. As previously stated, the energetic excesses in 2030 and 2050 are 64 TWh/year and 95.1 TWh/year respectively. In this regard, Fig. 7 provides a sensitivity analysis of the electrolyzer size, the hydrogen production costs (HPC), the system efficiency, and the capacity factor (CF) in 2030 and 2050. The X-axis represents the size of the electrolyzer to leverage the energy excesses for hydrogen generation, being "EL" the maximum size to obtain zero surpluses. It can be noted that harnessing all the excess electricity leads to the maximum efficiency of the system, 80 % in 2030 and 82 % in 2050. However, the production costs of the extra hydrogen generated are even higher than the base case (3.955 US$/kg for the base DIS3-PVSC scenario against 5.134 US$/kg of the extra production). This is due to the low capacity factor, calculated as the ratio between the average power of the electrolyzer and the maximum installed capacity, associated with the abrupt profile of energy excess. This value measures the degree of utilization of the electrolyzer. Therefore, we see that as the size of the electrolyzer decreases, the CF increases. On the other hand, part of the excess energy is no longer used, and thus, the overall efficiency of the installation decreases.

3.3.3. Extra energy storage capacity (2030 & 2050)

The design of combined renewables-hydrogen configurations implies the definition of a balance between direct RES consumption and energy storage in the form of hydrogen. The increase in direct RES consumption reduces the storage requirements, leading to faster filling of the storage systems and a corresponding increase in the energy excess. Hence, depending on the storage capacity availability it is possible to define suboptimal configurations that still achieve an LCOE below the Spanish utility grid benchmark. In this regard, as underground hydrogen storage in salt deposits accounts for a huge capacity, this section proposes to increase the storage capacity to dump the energy excess as much as possible and increase the overall system efficiency in the specific case of the DIS3-PVSC case study. Thus, direct RES consumption will decrease linked to the growth of storage. To carry out this analysis, the fuel cell and electrolyzer dimensions will remain constant and equal to DIS3-PVSC in both 2030 and 2050 to assess how much excess electricity could be reduced with the same hydrogen generation capacity.

Fig. 8 represents the variation on storage and RES capacity, excess energy, system efficiency, and LCOE with extra storage availability for DIS3-PVSC scenario. As depicted in the graph, a five-fold increase in stored hydrogen in salt deposits for both 2030 and 2050 results in a decrease in RES capacity, especially for PV parks that are halved by 2030 and reduced to less than one-third by 2050. On the other hand, wind turbines decrease from 47.8 GW to 36.8 GW in 2030, while in 2050 they

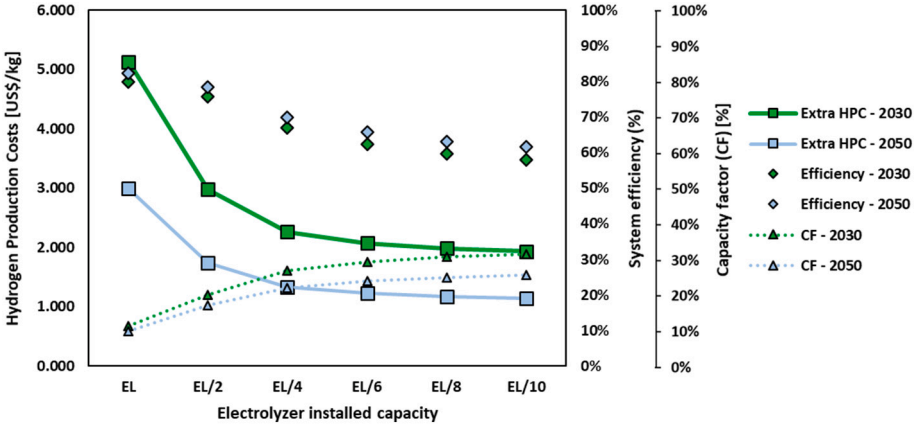

Fig. 7. Sensitivity analysis of electrolyzer size, hydrogen production costs (HPC), system efficiency, and capacity factor (CF) in 2030 and 2050 for DIS3-PVSC scenario.

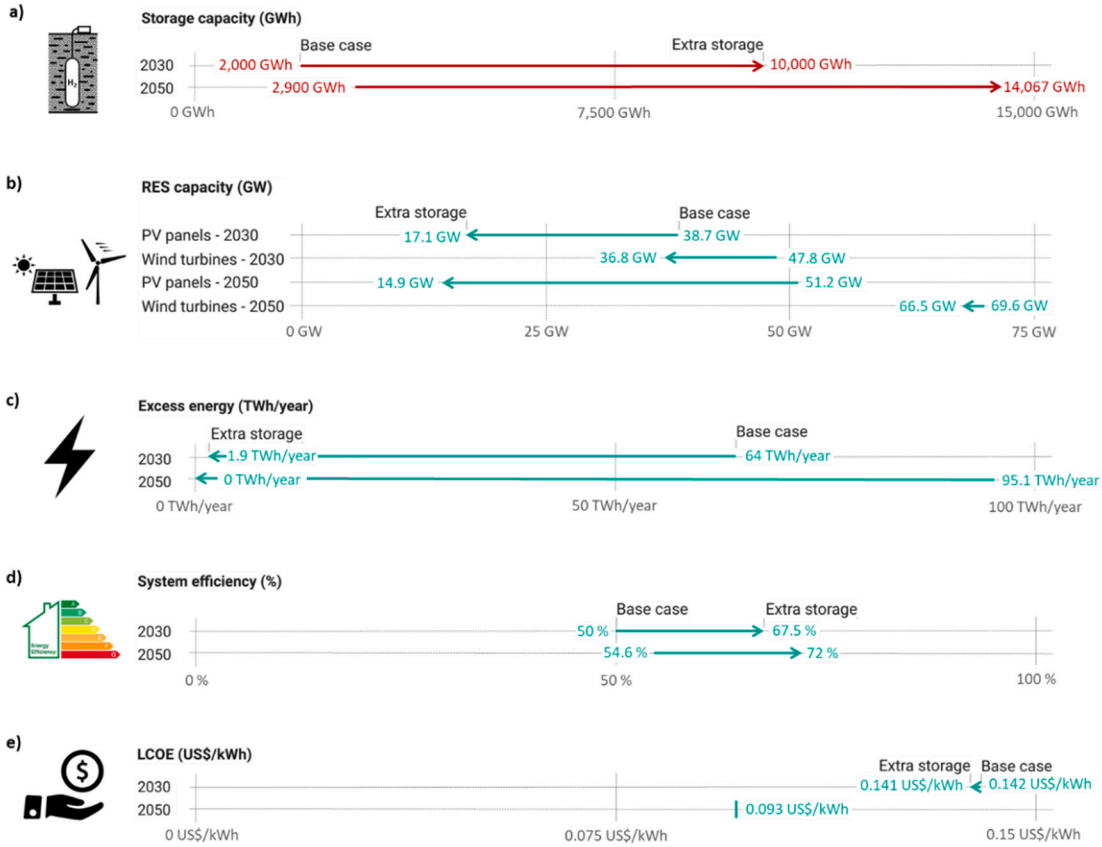

Fig. 8. Variation on a) storage and b) RES capacity, c) excess energy, d) system efficiency, and e) LCOE with extra storage availability for DIS3-PVSC scenario.

suffer a slight reduction of 3.1 GW from the initial value. The increase in storage capacity and the corresponding decrease in RES capacity influences the energy excess, leading to a reduction to 1.9 TWh/year in 2030. Furthermore, a complete removal of energy excess is achieved in 2050. On the other hand, the performance of the system improves by around 17.5 % for both time horizons. Finally, the variation on the LCOE is negligible as a slight reduction of 0.001 US$/kWh is achieved in 2030 and remains constant in 2050. Therefore, this alternative results in an interesting solution when having bulk hydrogen storage systems.

3.3.4. Excess energy for international exports (2030 & 2050)

Nowadays, international trading of energy and interconnections between countries are widely implemented. Particularly, Spain has strong electricity connections with the neighboring countries of Portugal, Andorra, and France. The latter country has a robust continuous supply based on nuclear energy. Therefore, France can be more suitable to purchase cheap RES excesses to fulfill energy requirements during peak periods. These RES excesses come from wind turbines and both rooftop and grounded PV panels, having a price of 0.0368 US $/kWh and 0.027 US$/kWh in 2030 and 2050 respectively. In this case, assuming that Spain sells extra electricity at these prices, it turns out in annual incomes of around 5 billion US$. Moreover, the final obtained costs of the energy are reduced from 0.142 US$/kWh to 0.095 US$/kWh in 2030, and from 0.093 US$/kWh to 0.053 US$/kWh.

4. Conclusions

This work analyzes the potential future decarbonization of the electricity demand of the Spanish building stock in 2030 and 2050 horizons through combined renewables-hydrogen configurations. To achieve this goal, different centralized and distributed scenarios of RES generation, hydrogen production, storage and re-electrification are evaluated. Moreover, not only the system dimensions are studied, but also the optimal locations selected through a land eligibility analysis.

Among the evaluated configurations, the combination of large renewable generation hubs and hydrogen production facilities, underground storage in salt caverns, and power retrieval in MW-scale fuel cells results as the most cost-effective solution for centralized scenarios in 2030 and 2050. In this regard, the deployment of self-consumption facilities based on rooftop PV panels and batteries along with the above configuration is the most favorable solution among the distributed case studies. In 2030, the CEN3-SC configuration reports a total renewable capacity of 84.5 GW, while DIS3-PVSC requires 74.4 GW to decarbonize the building sector. Likewise, the hydrogen chain is reduced from 26 GW of FC, 33 GW of EL, and 2100 GWh of hydrogen storage capacity for the CEN3-SC system to 19 GW of FC, 30 GW of EL, and 2000 GWh of hydrogen storage capacity for DIS3-PVSC in combination with 29 GWh of batteries. However, in 2050 the total renewable capacities for both scenarios slightly surpass 120 GW and the difference in electrolysis capacity is 1 GW. Concerning fuel cells, the DIS3-PVSC facility reports 11 GW less FC capacity required, as well as a reduction of around 300 GWh in hydrogen requirements thanks to batteries. These differences in the size imply a reduction in land utilization, that is further decrease due to the use of existing roofs to deploy PV panels. Moreover, end users could benefit from efficiency improvement subsidies in buildings, where PV self-consumption could be promoted, leading to additional revenues, the corresponding reduction of LCOE and HPC, and improvements in energy efficiency. Therefore, the DIS3-PVSC case study has been selected as the most promising configuration in the future.

Different solutions have been analyzed to convert energy surpluses into useful energy for other sectors such as industry, extra hydrogen production for transportation, the possibility of having additional storage potential, or incomes thanks to international energy trading. In this sense, the reinforcement of underground hydrogen reservoirs has been

proved the most advantageous solution, with deep reductions in RES deployment and great increases in overall efficiencies. In the case of Spain, with a huge potential of hydrogen storage in salt caverns, the development of this seasonal energy storage method will be key to boost energy transition towards a decarbonized electricity supply for the Spanish building stock.

The long-term decarbonization strategy and different roadmaps set by the government of Spain propose more than 120 GW of RES capacity installed and 42 % of RES contribution to total final energy consumed (TFEC) by 2030. Thus, the DIS3-PVSC scenario achieves a deployment of additional 74.7 GW that combined with the current 60 GW already installed in Spain exceeds the objective. Concerning the total final energy consumption, if we account for the total estimated electricity requirements of buildings in 2030 (162 TWh/year) and the total estimated electricity demand by Spain being 274 TWh/year, around 59.1 % of TFEC is provided by renewable energy sources which outperforms in 17 % the goal for 2030. This value can be increased if we consider storage reinforcement or utilization by other sectors. Therefore, these configurations will enable the accomplishment of the Spanish decarbonization objectives. However, 2050 decarbonization will require robust measures and cross-sectoral solutions to achieve a carbon-neutral economy. In the case of buildings, heating needs are fundamental. Therefore, the joint adoption of strategies integrating RES, hydrogen technologies, heat pumps, air heaters, and other efficiency measures will be required.

Declaration of competing interest

The authors declare that they have no known competing financial interests or personal relationships that could have appeared to influence the work reported in this paper.

Data availability

No data was used for the research described in the article.

Acknowledgments

This research is being supported by the Project ENERGY PUSH SOE3/P3/E0865, which is co-financed by the European Regional Development Fund (ERPF) in the framework of the INTERREG SUDOE Programme and the Spanish Ministry of Science, Innovation, and Universities (Projects RTI2018-093310-B-I00 and PLEC2021-007718).

Appendix A. Supplementary data

Supplementary data to this article can be found online at https://doi.org/10.1016/j.est.2022.105889.

References

[1] A. Foley, A.G. Olabi, Renewable energy technology developments, trends and policy implications that can underpin the drive for global climate change, Renew. Sust. Energ. Rev. 68 (2017) 1112–1114, https://doi.org/10.1016/j.rser.2016.12.065.
[2] N. McIlwaine, A.M. Foley, D.J. Morrow, D.Al Kez, C. Zhang, X. Lu, R.J. Best, A state-of-the-art techno-economic review of distributed and embedded energy storage for energy systems, Energy. (2021) 120461, https://doi.org/10.1016/j.energy.2021.120461.
[3] A. Mazza, E. Bompard, G. Chicco, Applications of power to gas technologies in emerging electrical systems, Renew. Sust. Energ. Rev. 92 (2018) 794–806, https://doi.org/10.1016/j.rser.2018.04.072.
[4] D. Parra, L. Valverde, F.J. Pino, M.K. Patel, A review on the role, cost and value of hydrogen energy systems for deep decarbonisation, Renew. Sust. Energ. Rev. 101 (2019) 279–294, https://doi.org/10.1016/j.rser.2018.11.010.
[5] E. Taibi, R. Miranda, W. Vanhoudt, T. Winkel, J.-C. Lanoix, F. Barth, Hydrogen from renewable power: Technology outlook for the energy transition, 2018. www.irena.org. (Accessed 10 July 2022).
[6] M. Yáñez, A. Ortiz, B. Brunaud, I.E. Grossmann, I. Ortiz, Contribution of upcycling surplus hydrogen to design a sustainable supply chain: the case study of northern Spain, Appl. Energy 231 (2018) 777–787, https://doi.org/10.1016/j.apenergy.2018.09.047.
[7] R. Ortiz-Imedio, A. Ortiz, J.C. Urroz, P.M. Diéguez, D. Gorri, L.M. Gandía, I. Ortiz, Comparative performance of coke oven gas, hydrogen and methane in a spark ignition engine, Int. J. Hydrog. Energy 46 (2021) 17572–17586, https://doi.org/10.1016/j.ijhydene.2019.12.165.
[8] IEA, Technology Roadmap: Hydrogen and Fuel Cells., 2015. www.iea.org/t&c/. (Accessed 22 July 2022).
[9] M. Yáñez, A. Ortiz, B. Brunaud, I.E. Grossmann, I. Ortiz, The use of optimization tools for the hydrogen circular economy, comput. Aided, Chem. Eng. 46 (2019) 1777–1782, https://doi.org/10.1016/B978-0-12-818634-3.50297-6.
[10] The SBC Energy Institute, Hydrogen-Based Energy Conversion, System Flexibility, More than Storage, 2014 http://www.sbc.slb.com/SBCInstitute.aspx, (accessed July 22, 2022).
[11] Iea, The future of hydrogen, Seizing today's opportunities, 2019.
[12] D.G. Caglayan, H.U. Heinrichs, M. Robinius, D. Stolten, Robust design of a future 100% renewable european energy supply system with hydrogen infrastructure, Int. J. Hydrog. Energy 46 (2021) 29376–29390, https://doi.org/10.1016/j.ijhydene.2020.12.197.
[13] M. Moser, H.C. Gils, G. Pivaro, A sensitivity analysis on large-scale electrical energy storage requirements in Europe under consideration of innovative storage technologies, J. Clean. Prod. 269 (2020), 122261, https://doi.org/10.1016/J.JCLEPRO.2020.122261.
[14] M. Pavičević, A. Mangipinto, W. Nijs, F. Lombardi, K. Kavvadias, J.P. Jiménez Navarro, E. Colombo, S. Quoilin, The potential of sector coupling in future european energy systems: soft linking between the dispa-SET and JRC-EU-TIMES models, Appl. Energy 267 (2020), 115100, https://doi.org/10.1016/J.APENERGY.2020.115100.
[15] M. Child, C. Kemfert, D. Bogdanov, C. Breyer, Flexible electricity generation, grid exchange and storage for the transition to a 100% renewable energy system in Europe, Renew. Energy 139 (2019) 80–101, https://doi.org/10.1016/J.RENENE.2019.02.077.
[16] K. Löffler, T. Burandt, K. Hainsch, P.Y. Oei, Modeling the low-carbon transition of the european energy system - a quantitative assessment of the stranded assets problem, Energy Strateg. Rev. 26 (2019), 100422, https://doi.org/10.1016/J.ESR.2019.100422.
[17] W. Zappa, M. Junginger, M. van den Broek, Is a 100% renewable european power system feasible by 2050? Appl. Energy 233–234 (2019) 1027–1050, https://doi.org/10.1016/J.APENERGY.2018.08.109.
[18] L. Welder, D.S. Ryberg, L. Kotzur, T. Grube, M. Robinius, D. Stolten, Spatio-temporal optimization of a future energy system for power-to-hydrogen applications in Germany, Energy 158 (2018) 1130–1149, https://doi.org/10.1016/J.ENERGY.2018.05.059.
[19] F. Grüger, O. Hoch, J. Hartmann, M. Robinius, D. Stolten, Optimized electrolyzer operation: employing forecasts of wind energy availability, hydrogen demand, and electricity prices, Int. J. Hydrog. Energy (2019) 4387–4397, https://doi.org/10.1016/J.IJHYDENE.2018.07.165.
[20] M. Reuß, T. Grube, M. Robinius, P. Preuster, P. Wasserscheid, D. Stolten, Seasonal storage and alternative carriers: a flexible hydrogen supply chain model, Appl. Energy 200 (2017) 290–302, https://doi.org/10.1016/J.APENERGY.2017.05.050.
[21] G. Guandalini, M. Robinius, T. Grube, S. Campanari, D. Stolten, Long-term power-to-gas potential from wind and solar power: a country analysis for Italy, Int. J. Hydrog. Energy 42 (2017) 13389–13406, https://doi.org/10.1016/J.IJHYDENE.2017.03.081.
[22] S. Samsatli, I. Staffell, N.J. Samsatli, Optimal design and operation of integrated wind-hydrogen-electricity networks for decarbonising the domestic transport sector in Great Britain, Int. J. Hydrog. Energy 41 (2016) 447–475, https://doi.org/10.1016/J.IJHYDENE.2015.10.032.
[23] S. Samsatli, N.J. Samsatli, The role of renewable hydrogen and inter-seasonal storage in decarbonising heat – comprehensive optimisation of future renewable energy value chains, Appl. Energy 233–234 (2019) 854–893, https://doi.org/10.1016/j.apenergy.2018.09.159.
[24] O. Tlili, C. Mansilla, M. Robinius, K. Syranidis, M. Reuss, J. Linssen, J. André, Y. Perez, D. Stolten, Role of electricity interconnections and impact of the geographical scale on the french potential of producing hydrogen via electricity surplus by 2035, Energy 172 (2019) 977–990, https://doi.org/10.1016/J.ENERGY.2019.01.138.
[25] J. Heras, M. Martín, Multiscale analysis for power-to-gas-to-power facilities based on energy storage, Comput. Chem. Eng. 144 (2021), https://doi.org/10.1016/j.compchemeng.2020.107147.
[26] P.M. Heuser, D.S. Ryberg, T. Grube, M. Robinius, D. Stolten, Techno-economic analysis of a potential energy trading link between Patagonia and Japan based on CO2 free hydrogen, Int. J. Hydrog. Energy 44 (2019) 12733–12747, https://doi.org/10.1016/J.IJHYDENE.2018.12.156.
[27] D.S. Ryberg, M. Robinius, D. Stolten, Methodological framework for determining the land eligibility of renewable energy sources, ArXiv. (2017) 1–35.
[28] D.S. Ryberg, D.G. Caglayan, S. Schmitt, J. Linßen, D. Stolten, M. Robinius, The future of european onshore wind energy potential: detailed distribution and simulation of advanced turbine designs, Energy 182 (2019) 1222–1238, https://doi.org/10.1016/j.energy.2019.06.052.
[29] D.S. Ryberg, Z. Tulemat, D. Stolten, M. Robinius, Uniformly constrained land eligibility for onshore european wind power, Renew. Energy 146 (2020) 921–931, https://doi.org/10.1016/j.renene.2019.06.127.
[30] D. Yassuda Yamashita, I. Vechiu, J.P. Gaubert, S. Jupin, Autonomous observer of hydrogen storage to enhance a model predictive control structure for building microgrids, J. Energy Storage. 53 (2022), 105072, https://doi.org/10.1016/J.EST.2022.105072.

[31] P. Marocco, D. Ferrero, A. Lanzini, M. Santarelli, The role of hydrogen in the optimal design of off-grid hybrid renewable energy systems, J. Energy Storage. 46 (2022), https://doi.org/10.1016/J.EST.2021.103893.

[32] M. Rezaei, U. Dampage, B.K. Das, O. Nasif, P.F. Borowski, M.A. Mohamed, Investigating the Impact of Economic Uncertainty on Optimal Sizing of Grid-Independent Hybrid Renewable Energy Systems, Process. 9 (2021) 1468, https://doi.org/10.3390/PR9081468, 9 (2021) 1468.

[33] T.D. Hutty, S. Dong, S. Brown, Suitability of energy storage with reversible solid oxide cells for microgrid applications, Energy Convers. Manag. 226 (2020), https://doi.org/10.1016/j.enconman.2020.113499.

[34] V.T. Giap, Y.S. Kim, Y.D. Lee, K.Y. Ahn, Waste heat utilization in reversible solid oxide fuel cell systems for electrical energy storage: fuel recirculation design and feasibility analysis, J. Energy Storage. 29 (2020), 101434, https://doi.org/10.1016/j.est.2020.101434.

[35] M. Wei, G. Levis, A. Mayyas, Reversible Fuel Cell Cost Analysis, 2020.

[36] V.M. Maestre, A. Ortiz, I. Ortiz, The role of hydrogen-based power systems in the energy transition of the residential sector, J. Chem. Technol. Biotechnol. (2021), https://doi.org/10.1002/JCTB.6938.

[37] V.M. Maestre, A. Ortiz, I. Ortiz, Challenges and prospects of renewable hydrogen-based strategies for full decarbonization of stationary power applications, Renew. Sust. Energ. Rev. 152 (2021), 111628, https://doi.org/10.1016/j.rser.2021.111628.

[38] G. Correa, F. Volpe, P. Marocco, P. Muñoz, T. Falagüerra, M. Santarelli, Evaluation of levelized cost of hydrogen produced by wind electrolysis: argentine and italian production scenarios, J. Energy Storage. 52 (2022), https://doi.org/10.1016/J.EST.2022.105014.

[39] P.T. Aakko-Saksa, C. Cook, J. Kiviaho, T. Repo, Liquid organic hydrogen carriers for transportation and storing of renewable energy – review and discussion, J. Power Sources 396 (2018) 803–823, https://doi.org/10.1016/J.JPOWSOUR.2018.04.011.

[40] R. Ströbel, J. Garche, P.T. Moseley, L. Jörissen, G. Wolf, Hydrogen storage by carbon materials, J. Power Sources 159 (2006) 781–801, https://doi.org/10.1016/J.JPOWSOUR.2006.03.047.

[41] J.D.O. Williams, J.P. Williamson, D. Parkes, D.J. Evans, K.L. Kirk, N. Sunny, E. Hough, H. Vosper, M.C. Akhurst, Does the United Kingdom have sufficient geological storage capacity to support a hydrogen economy? Estimating the salt cavern storage potential of bedded halite formations, J. Energy Storage. 53 (2022), 105109, https://doi.org/10.1016/J.EST.2022.105109.

[42] S.R. Thiyagarajan, H. Emadi, A. Hussain, P. Patange, M. Watson, A comprehensive review of the mechanisms and efficiency of underground hydrogen storage, J. Energy Storage. 51 (2022), https://doi.org/10.1016/J.EST.2022.104490.

[43] X. Cheng, Z. Shi, N. Glass, L. Zhang, J. Zhang, D. Song, Z.S. Liu, H. Wang, J. Shen, A review of PEM hydrogen fuel cell contamination: impacts, mechanisms, and mitigation, J. Power Sources 165 (2007) 739–756, https://doi.org/10.1016/J.JPOWSOUR.2006.12.012.

[44] E. Qu, X. Hao, M. Xiao, D. Han, S. Huang, Z. Huang, S. Wang, Y. Meng, Proton exchange membranes for high temperature proton exchange membrane fuel cells: challenges and perspectives, J. Power Sources 533 (2022), 231386, https://doi.org/10.1016/J.JPOWSOUR.2022.231386.

[45] MITECO, Estrategia a Largo Plazo Para Una Economía Española Moderna, Competitiva Y Climáticamente Neutra En 2050, Miteco. (2020) 73. https://www.miteco.gob.es/es/prensa/documentoelp_tcm30-516109.pdf.

[46] Consumos del Sector Residencial en España, 2021.

[47] HOMER Pro - Microgrid Software for Designing Optimized Hybrid Microgrids, (n.d.). https://www.homerenergy.com/products/pro/index.html (accessed July 9, 2022).

[48] A. Razmjoo, L. Gakenia Kaigutha, M.A. Vaziri Rad, M. Marzband, A. Davarpanah, M. Denai, A technical analysis investigating energy sustainability utilizing reliable renewable energy sources to reduce CO2 emissions in a high potential area, renew, Energy 164 (2021) 46–57, https://doi.org/10.1016/j.renene.2020.09.042.

[49] H. Mehrjerdi, H. Saboori, S. Jadid, Power-to-gas utilization in optimal sizing of hybrid power, water, and hydrogen microgrids with energy and gas storage, J. Energy Storage. 45 (2022), https://doi.org/10.1016/J.EST.2021.103745.

[50] C. Ghenai, M. Bettayeb, Optimized design and control of an off grid solar PV/hydrogen fuel cell power system for green buildings, IOP Conf. Ser. Earth Environ. Sci. 93 (2017), https://doi.org/10.1088/1755-1315/93/1/012073.

[51] D.N. Luta, A.K. Raji, Optimal sizing of hybrid fuel cell-supercapacitor storage system for off-grid renewable applications, Energy 166 (2019) 530–540, https://doi.org/10.1016/j.energy.2018.10.070.

[52] S. Peláez-Peláez, A. Colmenar-Santos, C. Pérez-Molina, A.E. Rosales, E. Rosales-Asensio, Techno-economic analysis of a heat and power combination system based on hybrid photovoltaic-fuel cell systems using hydrogen as an energy vector, Energy 224 (2021), https://doi.org/10.1016/j.energy.2021.120110.

[53] M.H. Jahangir, F. Javanshir, A. Kargarzadeh, Economic analysis and optimal design of hydrogen/diesel backup system to improve energy hubs providing the demands of sport complexes, Int. J. Hydrog. Energy (2021), https://doi.org/10.1016/j.ijhydene.2021.01.187.

[54] H. Rezk, E.T. Sayed, M. Al-Dhaifallah, M. Obaid, A.H.M. El-Sayed, M. A. Abdelkareem, A.G. Olabi, Fuel cell as an effective energy storage in reverse osmosis desalination plant powered by photovoltaic system, Energy 175 (2019) 423–433, https://doi.org/10.1016/j.energy.2019.02.167.

[55] M. Ansong, L.D. Mensah, M.S. Adaramola, Techno-economic analysis of a hybrid system to power a mine in an off-grid area in Ghana, Sustain. Energy Technol. Assessments. 23 (2017) 48–56, https://doi.org/10.1016/j.seta.2017.09.001.

[56] GitHub - FZJ-IEK3-VSA/glaes: Geospatial Land Availability for Energy Systems, (n.d.). https://github.com/FZJ-IEK3-VSA/glaes (accessed July 17, 2022).

[57] D.S. Ryberg, M. Robinius, D. Stolten, Evaluating land eligibility constraints of renewable energy sources in Europe, Energies. 11 (2018) 1–19, https://doi.org/10.3390/en11051246.

[58] D.S. Ryberg, Z. Tulemat, D. Stolten, M. Robinius, Uniformly constrained land eligibility for onshore european wind power, Renew. Energy 146 (2020) 921–931, https://doi.org/10.1016/J.RENENE.2019.06.127.

[59] Balance del Consumo de energía final, (n.d.). https://sieeweb.idae.es/consumofinal/bal.asp?txt=Residencial&tipbal=s&rep=1 (accessed June 29, 2022).

[60] bp Statistical Review of World bp, Energy (2020) (accessed June 23, 2022), www.bp.com/statisticalreview.

[61] P. Linares, D. Declercq, Escenarios para el sector energético en España 2030–2050 (2017) 1–80.

[62] Irena, The Power to Change: Solar and Wind Cost Reduction Potential to 2025, 2016. www.irena.org. (Accessed 11 July 2022).

[63] IEA Trends in Photovoltaic Applications, 2020. www.iea-pvps.org, 2020 accessed July 22, 2021.

[64] A. Walker, E. Lockhart, J. Desai, K. Ardani, G. Klise, O. Lavrova, T. Tansy, J. Deot, B. Fox, A. Pochiraju, Model of Operation-and-Maintenance Costs for Photovoltaic Systems, 2020. https://www.nrel.gov/docs/fy20osti/74840.pdf. (Accessed 16 February 2022).

[65] (accessed July 11, 2022).

[66] R. Wiser, K. Jenni, J. Seel, E. Baker, M. Hand, E. Lantz, A. Smith, V. Berkhout, A. Duffy, B. Cleary, R. Lacal-Arántegui, L. Husabø, J. Lemming, S. Lüers, A. Mast, W. Musial, B. Prinsen, K. Skytte, G. Smart, B. Smith, B. Sperstad, P. Veers, A. Vitina, D. Weir, Forecasting Wind Energy Costs and Cost Drivers: The Views of the World's Leading Experts (2016).

[67] T.R.A.C.T.E.B.E.L. ENGIE, Study on early business cases for H2 in energy storage and more broadly power to H2 applications, 2017..

[68] F.C.H. Ju, Advancing Europe's energy systems: Stationary fuel cells in distributed generation (2015), https://doi.org/10.2843/088142.

[69] IRENA, Green hydrogen cost reduction: scaling up electrolysers to meet the 1.5oC climate goal, 2020. www.irena.org/publications. (Accessed 29 July 2022).

[70] R.K. Ahluwalia, D.D. Papadias, J.-K. Peng, H.S. Roh, System Level Analysis of Hydrogen Storage Options, 2019.

[71] U. Energy, Information Administration, Battery Storage in the United States: An Update on Market Trends, 2021. www.eia.gov. (Accessed 20 July 2022).

[72] NREL, Hydrogen Station Compression, Storage, and Dispensing Technical Status and Costs: Systems Integration, 2014. http://www.osti.gov/bridge. (Accessed 13 July 2022).

[73] Hydrohub Innovation Program, Gigawatt green hydrogen plant, 2020. https://ec.europa.eu/commission/presscorner/detail/en/ip_20_1259. (Accessed 22 July 2022).

[74] Q. Chen, Y. Gu, Z. Tang, D. Wang, Q. Wu, Optimal design and techno-economic assessment of low-carbon hydrogen supply pathways for a refueling station located in Shanghai, Energy 237 (2021), https://doi.org/10.1016/J.ENERGY.2021.121584.

[75] Hydrogen Delivery Scenario Analysis Model, (n.d.). https://hdsam.es.anl.gov/index.php?content=hdsam. (Accessed 4 August 2022).

[76] S.S. Makridis, Hydrogen storage and compression, (n.d.).

[77] IEA, The Role of Critical Minerals in Clean Energy Transitions, n.d. www.iea.org/t&c/ (accessed June 22, 2022).

[78] Ministerio para la Transición Ecológica y el Reto Demográfico, Plan nacional Integrado de Energía y Clima, 2021.

[79] IEA, Global Hydrogen Review 2021, 2022. www.iea.org/t&c/. (Accessed 26 July 2022).

[80] (accessed July 30, 2022).

[81] Electricity prices for households around the world, (n.d.). https://www.globalpetrolprices.com/electricity_prices/#hl160 (accessed July 27, 2022).

[82] HYUNDER project., (2012). http://hyunder.eu/ (accessed July 22, 2022).

[83] D.G. Caglayan, N. Weber, H.U. Heinrichs, J. Linßen, M. Robinius, P.A. Kukla, D. Stolten, Technical potential of salt caverns for hydrogen storage in Europe, Int. J. Hydrog. Energy 45 (2020) 6793–6805, https://doi.org/10.1016/j.ijhydene.2019.12.161.

[84] H. Blanco, A. Faaij, A review at the role of storage in energy systems with a focus on power to gas and long-term storage, Renew. Sust. Energ. Rev. 81 (2018) 1049–1086, https://doi.org/10.1016/j.rser.2017.07.062.

[85] M. Estratégico De Energía, Y. Clima, HOJA DE RUTA DEL AUTOCONSUMO, (n.d.).